Mat. Res. Soc. Symp. Proc. Vol. 612 © 2000 Materials Research Society

Probing Pore Characteristics in Low-K Thin Films Using Positronium Annihilation Lifetime Spectroscopy

D. W. Gidley, W. E. Frieze, T. L. Dull[1], J. N. Sun[1], and A. F. Yee[1]
Department of Physics, University of Michigan, Ann Arbor, MI 48109
[1]Department of Materials Science and Engineering, University of Michigan, Ann Arbor, MI 48109

ABSTRACT

Depth profiled positronium annihilation lifetime spectroscopy (PALS) has been used to probe the pore characteristics (size, distribution, and interconnectivity) in thin, porous films, including silica and organic-based films. The technique is sensitive to all pores (both interconnected and closed) in the size range from 0.3 nm to 300 nm, even in films buried under a diffusion barrier. PALS may be particularly useful in deducing the pore-size distribution in closed-pore systems where gas absorption methods are not available. In this technique a focussed beam of several keV positrons forms positronium (Ps, the electron-positron bound state) with a depth distribution that depends on the selected positron beam energy. Ps inherently localizes in the pores where its natural (vacuum) annihilation lifetime of 142 ns is reduced by collisions with the pore surfaces. The collisionally reduced Ps lifetime is correlated with pore size and is the key feature in transforming a Ps lifetime distribution into a pore size distribution. In thin silica films that have been made porous by a variety of methods the pores are found to be interconnected and an average pore size is determined. In a mesoporous methyl-silsesquioxane film with nominally closed pores a pore size distribution has been determined. The sensitivity of PALS to metal overlayer interdiffusion is demonstrated. PALS is a non-destructive, depth profiling technique with the only requirement that positrons can be implanted into the porous film where Ps can form.

INTRODUCTION

There is currently a great deal of interest in introducing and characterizing nanometer-sized voids into thin silica and polymer films. Such porous films are being intensely pursued by the microelectronics industry as a strategy for reducing the dielectric constant of interlayer insulators in microelectronic devices. Unfortunately, there are relatively few techniques capable of probing the pore characteristics (average size, size distribution, and interconnectivity) in sub-micron films on thick substrates. This is particularly true if the voids are closed (not interconnected) so that gas absorption techniques are not available. Transmission electron microscope (TEM) images, for example, are inherently challenging to interpret in such amorphous insulators. Neutron scattering [1] and beam-based positronium annihilation lifetime spectroscopy (PALS) [2] have recently been used to determine an average pore size in silica films and beam-based Doppler broadening positron annihilation spectroscopy [3] has been used to probe open-volume in silsesquioxane films. In closed-pore systems PALS may be uniquely capable of deducing a pore-size *distribution* [4], even in films buried under diffusion barriers. In this paper we will review the methodology and recent results of PALS.

PALS EXPERIMENTAL TECHNIQUE

In using PALS with thin films, an electrostatically focused beam of several keV positrons is generated in a high vacuum system using a radioactive beta-decay source of ^{22}Na (Figure 1). This beam is deflected onto a target sample as shown in the inset to this figure and forms positronium (Ps, the electron-positron bound state) throughout the film thickness. Positrons striking the sample generate secondary electrons that are detected in a channel plate (CEMA) and the Ps lifetime for each event is the time between this CEMA signal and the subsequent detection of annihilation gamma rays in a plastic scintillator. Ps inherently localizes in the pores where its natural annihilation lifetime of 142 ns is reduced by annihilation with molecular electrons during collisions with the pore surface. The collisionally reduced Ps lifetime is correlated with void size and forms the basis of the technique.

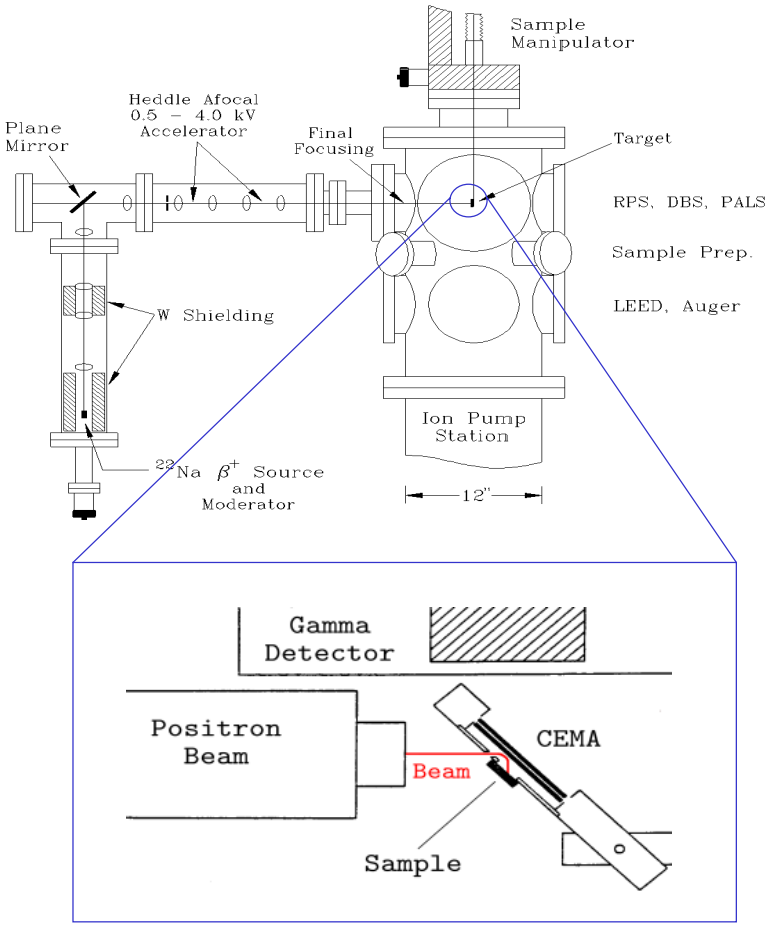

Figure 1. Schematic of the Depth-Profiled Positron Spectrometer.

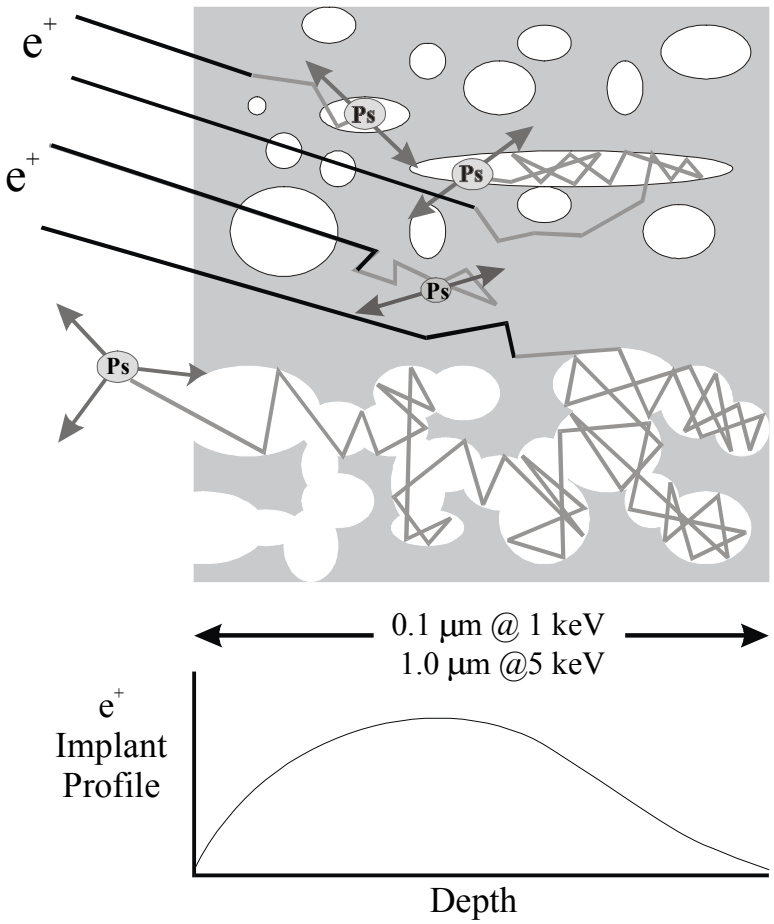

Figure 2. Positronium formation in porous materials. The shape of a typical positron implantation profile is depicted in the lower panel.

The formation of Ps in a porous insulator is depicted in Figure 2. The positron slows down through collisions in the material from its initial beam energy of several keV to several eV. It can either capture a bound molecular electron or recombine with free "spur" electrons generated by ionizing collisions to form the electron-positron bound state of positronium, Ps. This Ps, which initially has a few eV of kinetic energy, begins to diffuse and thermalize in the insulator. In porous films it localizes in the void volume where the Ps binding energy is not reduced by the dielectric constant of the surrounding material. However, even when it is thermalized in the pores, Ps is still colliding with the pore walls and the resulting Ps lifetime is shortened by positron annihilation with molecularly bound electrons in addition to the captured electron. Furthermore, Ps may diffuse over long distances that can be greater than the porous film thickness if the pores are interconnected. As a result Ps can easily diffuse out of the film and into the surrounding vacuum as depicted in Figure 2. The observable effect on the Ps lifetime is that most of the Ps annihilates with the vacuum lifetime of 142 ns, a telltale indicator that the pores in the film are interconnected. This is what we have found so far [2] for all porous silica films, regardless of manufacturing process. They have interconnected pores and Ps diffuses within the pore volume with most Ps finding its way into the vacuum. To extract information on the average pore size (technically, the mean free path for Ps in the interconnected pores) it is

necessary to deposit a thin capping layer on top of the film to keep the Ps corralled in the porous film. Examples of lifetime spectra acquired with an aluminum-capped and an uncapped porous silica film are shown in Figure 3. The effect of the Ps diffusion barrier is clearly evident. In this example the 41 ns lifetime acquired in the capped film is the correct, collisionally-shortened lifetime to associate with Ps in the pores. Thus PALS gives a clear indication of pore interconnectivity and, once the film is capped, a single lifetime component corresponding to the average mean free path of Ps throughout the entire film is fitted.

If the pores are closed (as depicted in the upper part of Figure 2) then Ps should be trapped in a pore with no further diffusion occurring. Indeed, in such materials no capping layer is required. Furthermore, a distribution of Ps lifetimes may result if there is a distribution of pore sizes. Deconvolution of a pore size distribution from a Ps lifetime distribution is one goal of our research and will be considered after discussion of the lifetime vs. pore size calibration.

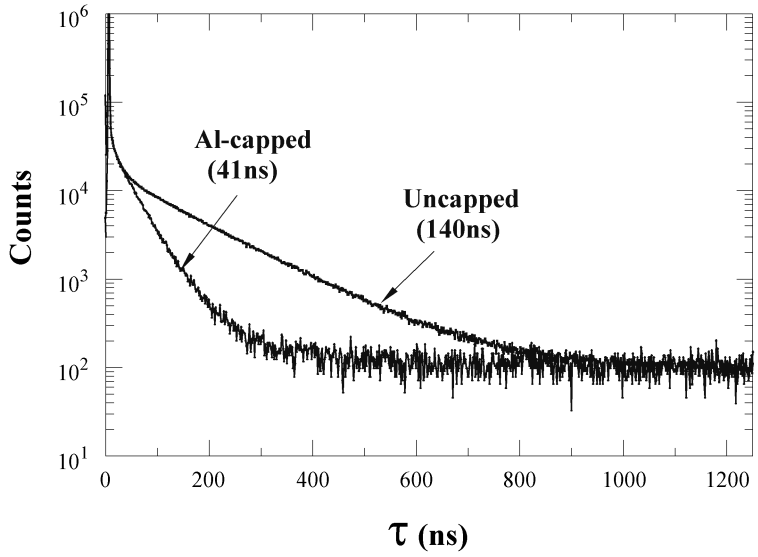

Figure 3. PALS spectra of uncapped and Al-capped porous silica films.

Calibration of Pore Size and Open Pore Systems

It is important to calibrate Ps lifetimes with pore sizes. In the very large pore (classical) regime (pores with mean free paths of order 100 nm), calibration was performed using high porosity (90-98%) silica powders [5]. In the other extreme (sub-nm pores), the quantum mechanical model first developed by Tao [6] and Eldrup [7] has been empirically used to calibrate Ps lifetimes of several nanoseconds with pore size, such as those in polymers [8]. In this simple model Ps is localized in a spherical infinitely deep potential well and only annihilates with molecular electrons when it is within a short distance of the pore surface. With only the ground state of Ps being considered in this Tao-Eldrup model, it is insufficient for characterizing larger voids where the pore diameter approaches the thermal De Broglie wavelength of positronium (about 6nm). Thermally excited states of Ps atoms in the pore must be included in

the calculation. As a result, the effect of sample temperature should also appear in the calibration of lifetime versus pore size.

To fully extend the quantum mechanical model to the classical, large-pore limit, we have modified the Tao-Eldrup model in order to characterize both micro and mesopores. To summarize the results presented in Reference [2], a rectangular pore shape is assumed for calculational simplicity and it is assumed that there is no Ps-surface interaction. It is assumed that the Ps atoms randomly sample all of the states in the rectangular well with a probability governed by the Maxwell-Boltzman distribution. At a given temperature, a lifetime vs. pore dimension curve can then be calculated.

It is useful to convert such curves from rectangular pore dimension to a classical mean-free path, $l=4V/S$, where V/S is the volume-to-surface area ratio of the rectangular pore used in the calculation. The mean-free path is a linear measure of pore size that is independent of pore geometry. Furthermore, in large (classical) pores the Ps lifetime depends only on the mean-free path. As will be shown below, even well into the quantum mechanical regime, the Ps lifetime depends almost entirely on the mean-free path and is only modestly dependent on the detailed pore geometry. For these reasons, and for calculational simplicity when deriving pore-size distributions in closed pore systems, it is desirable to work with the mean-free path as opposed to physical pore dimension.

Figure 4 shows lifetime vs. mean-free path curves at several different temperatures. Cubic pores were used in the calculations. The model includes only one fitting parameter that is determined by existing experimental data for l below 2 nm. At room temperature, the model extrapolates perfectly through precision measurements [5] in large-pore silica powders as shown. Ps lifetimes measured in bulk silica gels with pores calibrated by gas absorption methods are in quite reasonable agreement [9] with Figure 4, but display a large scatter. Recently, identical silica films were studied by small angle neutron scattering (SANS)[1] and by beam-PALS [2] and the deduced average cord/mean free path was 6.5 ± 0.1 nm and 7.5 ± 0.3 nm, respectively. Further agreement between PALS and SANS at the 15 nm size scale in porous poly (arylene ether) films will soon be reported, as will a comparison of PALS with a gas absorption technique

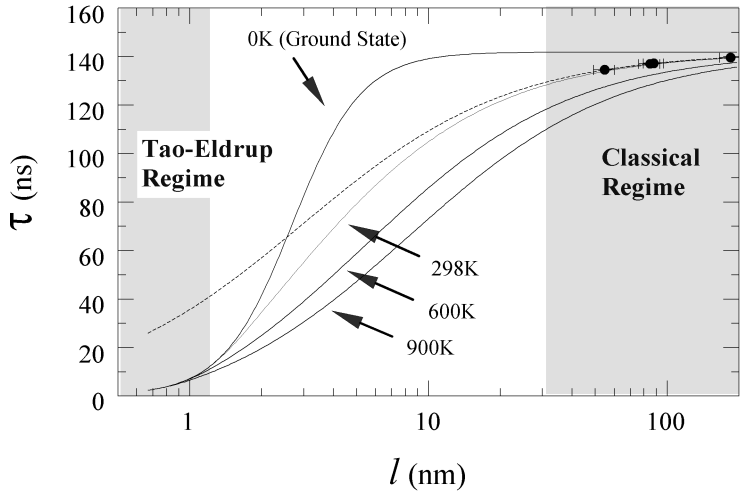

Figure 4. Pore-size calibration calculated at different temperatures using a cubical pore shape.

in a silica film with 3 nm-sized pores. These isolated comparisons suggest that our extension of the Tao-Eldrup model is valid and accurate for a range of materials. A systematic round robin of four identical sample films is presently underway to compare the results of PALS, SANS, ellipsometric porosimetry, gas absorption, and x-ray scattering. Results are to be presented during the conference.

The temperature dependence of the Ps lifetime, τ, was tested by PALS on several mesoporous samples and the very good agreement will be presented in the following sections (see also Figure 3 in Reference [2]). Note that all the calibrations of τ vs. pore size in this work are based on our theoretical extension of this model. To demonstrate the slight dependence on pore geometry, refer to Figure 5 in which Ps lifetime as a function of mean-free path has been plotted at two different temperatures using cubes and infinitely long square channels in the calculations.

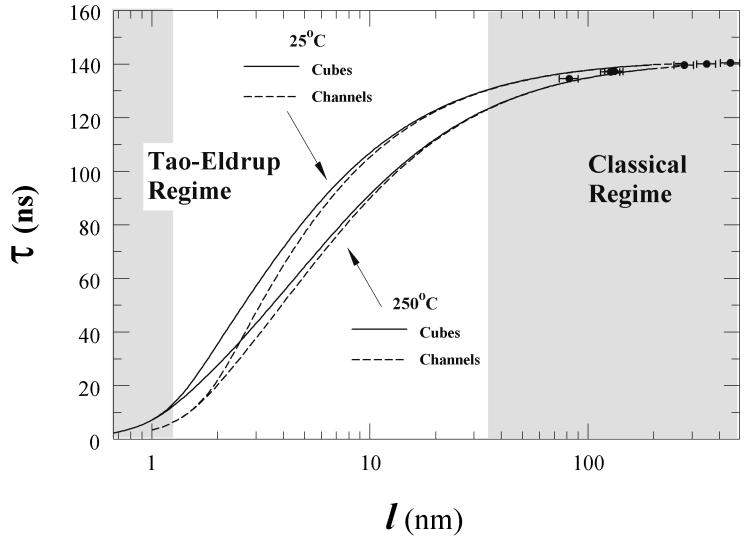

Figure 5. The effect of pore geometry at two sample temperatures.

Closed Pore Systems and Pore Size Distribution

The existence of closed pores with varying sizes should produce a distribution of Ps lifetimes since there is a singular relationship between pore size and τ indicated in the Tao-Eldrup model and our extension of it. This is the key feature that permits a PALS continuum lifetime distribution to be transformed into a pore-size distribution if Ps is trapped in isolated voids of varying sizes.

Our PALS study [4] on spin-on porous poly-MSSQ thin films clearly presents a distribution of lifetimes. These films were prepared by spin-casting a homogeneous mixture of methyl silsesquioxane prepolymers (Mn~1000 g/mol) and 6-arm poly-caprolactone (PCL). Upon heating the spin-on films to 250°C, cure reaction of MSSQ proceeded, during which phase separation occurred and PCL domains formed. The mesoporous films received from IBM were developed by ramping the cured poly-MSSQ/PCL films to 430°C and holding for 2hrs before cooling down to room temperature in house nitrogen, during which process, the PCL phase thermally decomposed and left behind pores. Lifetime spectra acquired before and after decomposition of

the PCL are compared in Figure 6. Initially we used the program POSFIT to fit discrete lifetimes to this spectrum. Prior to PCL decomposition the "unfoamed" film presents lifetimes consistent with those in bulk MSSQ (0.4 ns, 1.5 ns, and 6 ns), but no mesoporous lifetime components are observed. The fully decomposed porogen "foamed" sample shows long-lived events that cannot be adequately fitted with a single lifetime. At least two components (around 45 ns and 120 ns) are required in the fitting and the long lifetime component may be indicative of possible diffusion and escape of Ps into the vacuum. This suspicion was confirmed by spectra acquired with a 800 A sputter-deposited Al capping layer that confines Ps to the porous film. The 120 ns component disappeared as expected and lifetime components around 20 ns and 60 ns emerged, suggesting that only a portion of the pores are interconnected; a distribution of Ps lifetimes is still required for adequate fitting. Thus, these films may have a complicated, partially interconnected, pore system.

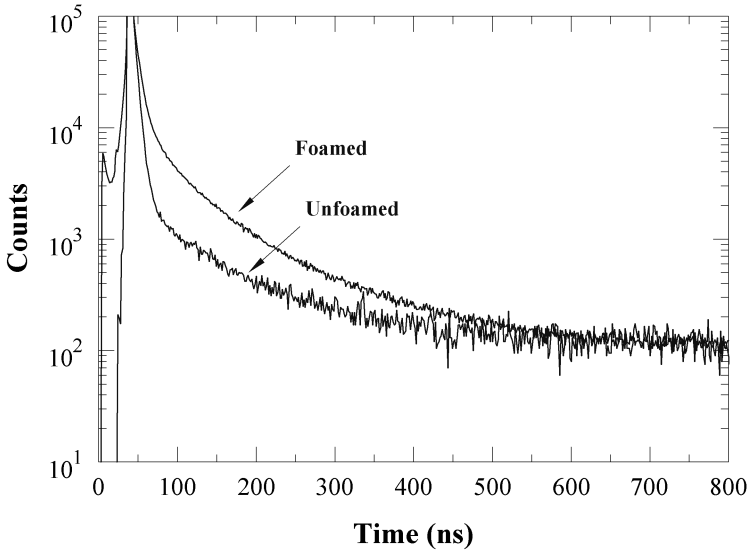

Figure 6. PALS spectra of foamed and unfoamed poly-MSSQ films.

The lifetime spectra shown in Figure 6 are given by dN_{Ps} / dt. To focus on the mesoporous part of the time spectrum we fit data for t beyond 60 ns, thus avoiding the bulk components with lifetimes less than 6 ns. We use a version of the continuum fitting program, CONTIN [10], specialized for exponential lifetime analysis. The result of this fitting program for the capped, fully-decomposed, film is shown in Figure 7 for two sample temperatures. (It should be noted the uniqueness of the fitted distributions presented in Figure 7 is still an open issue [4].) Given a statistically acceptable Ps lifetime distribution, $(1/N_{Ps})(dN_{Ps}/d\tau)$, determined from fitting the lifetime spectrum with CONTIN, the goal is to transform this distribution of Ps lifetimes into a distribution of void sizes, or more specifically, the specific void volume as a function of mean-free path. A key step in the transformation is a correction that must be made for Ps diffusing to and preferentially trapping in pores of large surface area. See Reference [4] for a detailed derivation. The fractional pore volume distribution as a function of mean-free path, l, is given by

$$\frac{1}{V}\frac{dV}{dl} = \frac{1}{N_{Ps}}\frac{dN_{Ps}}{d\tau}\frac{d\tau}{dl}l.$$

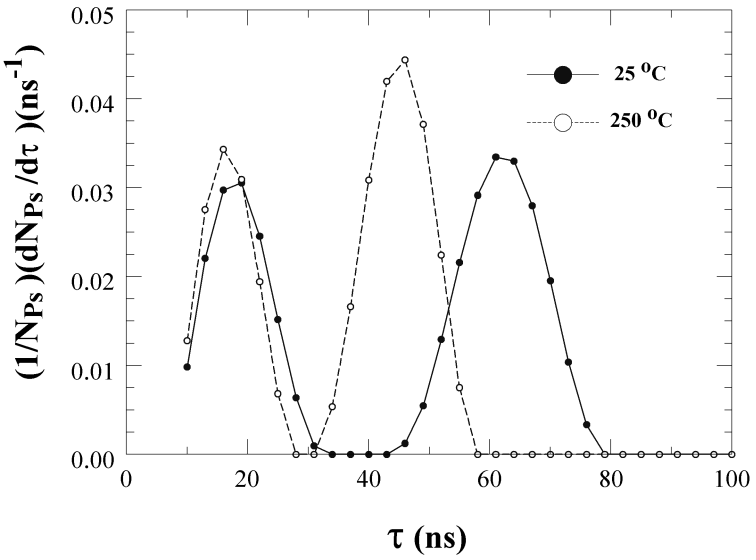

Figure 7 . Normalized Ps lifetime distribution (fitted using CONTIN) of the capped "foamed" poly-MSSQ film at 25C and 250C.

There is an inherent uncertainty in this distribution due to the slight dependence of Ps lifetime on the pore geometry. As shown in Figure 5, this effect is mainly confined to pores with mean free paths less than 2 nm.

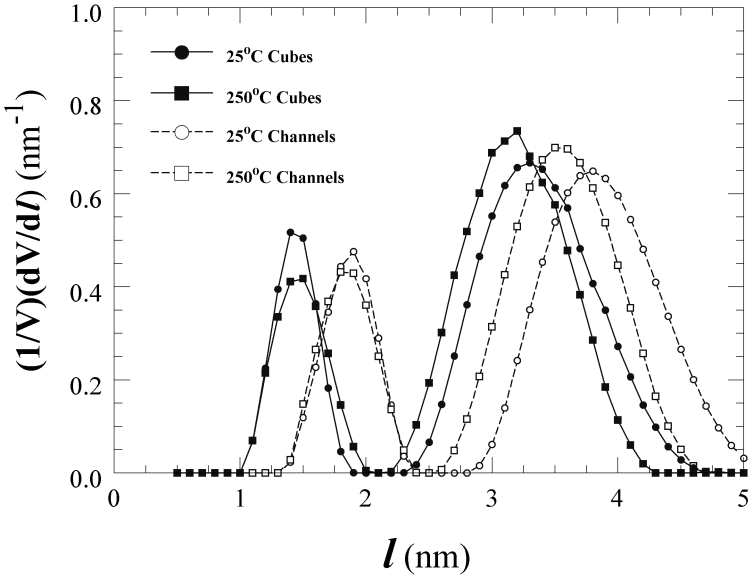

Figure 8. Volume fraction distribution in the mean free path, *l*, of a pore for spectra acquired at two different sample temperatures and analyzed using two different pore model dimensionalities.

Figure 8 shows the void volume distributions obtained from the lifetime distributions in Figure 7 using the calibrations of Figure 5. The solid symbols and curves correspond to the high and low temperature results derived using a closed, cubic pore model. The open symbols and

dashed curves are the same spectra analyzed using an infinitely long, square-channel pore model. Although the lifetime distributions in Figure 7 were acquired at two different temperatures and are therefore quite different, the deduced pore size distributions in Figure 8 are quite similar. This is an important systematic test of the model that demonstrates that Ps is thermally distributed throughout the entire void volume and not adsorbed on the void surface. The systematically larger pore sizes deduced using the channels as compared with the cubic pores is indicative of the typical systematic error that would be assigned in the determination of these distributions. Presumably, the "correct" distribution falls somewhere between these limiting cases of pore dimensionality. Given the uniqueness issues surrounding CONTIN fitting (mentioned above) and the fact that an electron micrograph presented in reference [4] could not fully substantiate the distributions in Figure 8, we recommend further research on this difficult deconvolution of pore size distribution.

Metal Interdiffusion Into the Porous Film and Diffusion Barrier Integrity

In addition to determining the average pore size in open pore systems and extracting a pore size distribution in closed pore systems, PALS can be used to study the integrity of diffusion barriers and the diffusion of metal overlayers into the porous film. In the process of studying an open-porosity silica film, we attempted to cap the film by depositing 800 Å of thermally evaporated aluminum without the use of any sample cooling. Instead of the 140 ns component being shortened to a 70 ns component indicative of Ps diffusing within the interconnected pore structure of the film, the long-lived component totally disappeared and a short, 3 ns, component appeared in its place. We confirmed that the sample warmed up during the deposition, resulting in aluminum diffusion into the pore structure. A metal coating on the pores would explain the appearance of the 3 ns component since Ps annihilation would be enhanced by the high density of free electrons. We verified that the silica film did indeed have a large open pore structure by room temperature sputter-deposition of an Al cap and fitting a single 70 ns lifetime component. These results are shown in Figure 9.

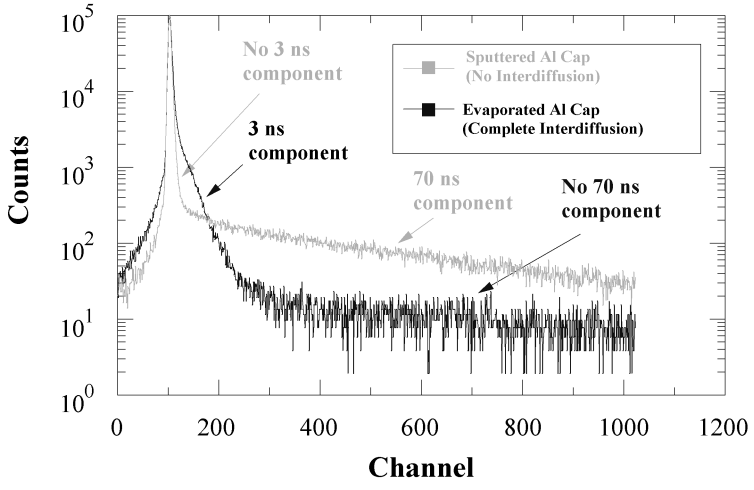

Figure 9. PALS spectra of identical silica films: one with a cold sputter-deposited Al cap and another that underwent uncontrolled heating during Al thermal evaporation.

To test the metal interdiffusion hypothesis we performed a systematically controlled study involving an Al sputter-capped silica film with an inherent lifetime component of 98 ns. We heat-treated the film at progressively higher temperatures and collected data at room temperature in between each heating cycle. We monitored the intensity of the 98 ns component and searched for the appearance of a short 3 ns lifetime component. The results are shown in Figure 10. At approximately 450 C we see the apparent onset of Al interdiffusion. This temperature is consistent with that of bulk annealing of Al and is probably significantly higher than that experienced by the sample during the thermal evaporation process. We tentatively conclude that the sample temperature during *vapor* deposition is much more critical than subsequent processing temperatures in preventing metal interdiffusion.

In a complementary study we are collaborating with SEMATECH to assess the integrity of candidate materials for use as thin diffusion barriers to prevent Cu and Al interdiffusion into the low-K films. Candidate materials are deposited with varying thicknesses as thin capping layers on silica films with interconnected pores. To qualify as a diffusion barrier *for Ps* such a capping layer must not allow any Ps to escape through the open silica pore structure into the vacuum (escape is readily manifested by a 140 ns component in the fitted PALS spectrum). Heat treatment of the film is also performed to test for thermal stability of the diffusion barrier. In this manner candidate materials and minimum critical barrier thickness can be identified. It is presumed that a diffusion barrier should at least be able to barrier Ps diffusion. However, other effects such as grain boundary diffusion of Cu atoms through a barrier will not be accounted for with Ps and would require separate testing.

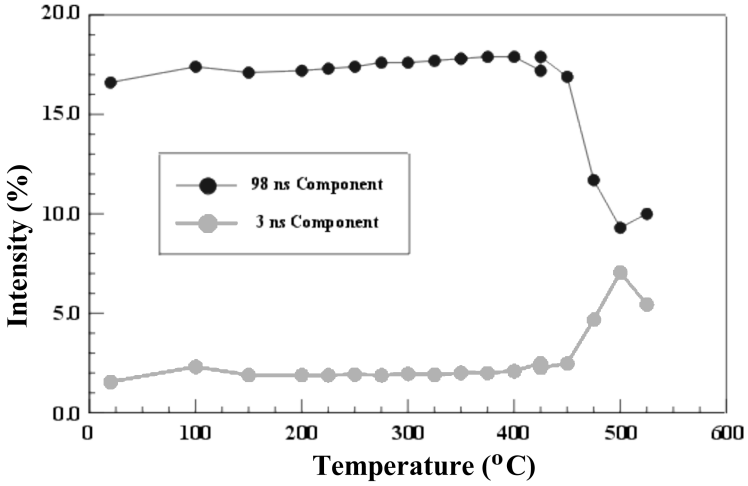

Figure 10. Controlled Al interdiffusion study using a silica film with a characteristic Ps lifetime of 98 ns within its interconnected pores.

CONCLUSION

PALS is a non-destructive, depth-profiling technique with the rather simple requirement that positrons can be implanted into the porous film where Ps can form. It is sensitive to *all* the void volume greater than a few angstroms in size, regardless of whether the pores are open or closed. The technique can readily distinguish open from closed porosity. In open (interconnected) pores a single Ps lifetime is fitted corresponding to the mean free path in the void volume throughout

the film thickness. In this case capping of the film is required to keep Ps from escaping into the vacuum. This property can also be exploited to test the integrity of candidate materials for diffusion barriers and determine critical barrier thicknesses. Metal interdiffusion into the open pores can also be observed since metal coating of the pore surfaces drastically reduces the Ps lifetime. In closed pores with varying sizes the PALS spectrum contains a distribution of Ps lifetimes that should correspond to the pore size distribution. Such a distribution of Ps lifetimes has definitely been observed and a pore shape independent method to deconvolve a fractional void volume distribution in mean free path has been proposed.

ACKNOWLEDGEMENTS

We thank Simon Lin, Todd Ryan, and Huei-Min Ho at SEMATECH and Do Yoon at Seoul National University for helpful discussions. Cattien Nguyen, formerly at IBM, prepared the mesoporous MSSQ films. Sputter-coating by David Beglau at ECD Inc. is gratefully acknowledged. This research is supported by NSF grant ECS–9732804 and by the Low-K Dielectric Program at SEMATECH.

REFERENCES

1. W. -L Wu, W. E. Wallace, E. K. Lin, G. W. Lynn, C. J. Glinka, E. T. Ryan and H. -M. Ho, *Appl. Phys.* **87**, 1193 (2000).
2. 2. D. W. Gidley, W. E. Frieze, A. F. Yee, T. L. Dull, E. T. Ryan, and H. –M. Ho*, Phys. Rev. B. **60** (Rapid Comm.),* R5157 (1999).
3. M. P. Petkov, M. H. Weber, K. G. Lynn, K. P. Rodbell, and S. A. Cohen, *J. Appl. Phys.* **86**, 3104 (1999).
4. D. W. Gidley, W. E. Frieze, T. L. Dull, J. Sun, A. F. Yee, C. V. Nguyen, and D. Y. Yoon, *Appl. Phys. Lett.* **76**, 1282 (2000).
5. D. W. Gidley, K. A. Marko, and A. Rich, *Phys. Rev. Lett.* **36,** 395 (1976).
6. S. J. Tao, *J. Chem. Phys.* **56**, 5499 (1972).
7. M. Eldrup, D. Lighbody, and J. N. Sherwood, *Chem. Phys.* **63**, 51 (1981).
8. Y. Y. Wang, Y. Nakanishi, Y. C. Jean, and T. C. Sandreczki*, J. Polym. Sci., Part B: Polym. Phys.* **28**, 1431 (1990).
9. K. Ito, H. Nakanishi, and Y. Ujihira*, J. Phys. Chem. B* **103**, 4555 (1999) and references therein.
10. S. W. Provencher, *Comput. Phys. Commun.* **27**, 213 (1982).